IRON AND OXYGEN ISOTOPE FRACTIONATION DURING PHOTO-OXIDATION. N. X. Nie[1], N. Dauphas[1] and R. C. Greenwood[2]. [1]Origins Lab, Department of the Geophysical Sciences and Enrico Fermi Institute, The University of Chicago, Chicago, IL 60637, USA (xike@uchicago.edu); [2]Planetary and Space Sciences, The Open Univeristy, Milton Keynes MK7 6AA, UK.

Introduction. Ultraviolet (UV) photochemical oxidation of aqueous ferrous iron ($Fe(II)_{aq}$) has been proposed as an effective pathway to the precipitation of banded iron formations (BIFs) [1, 2]. The rationale is that in the early Precambrian more high-energy UV sunlight could reach the seawater surface, because in absence of O_2, the atmosphere was more transparent to UVs. The other two possible alternatives are: (i) O_2-mediated oxidation, in which local "O_2 oasis" are created during photosynthesis by microorganisms such as cyanobacteria [3, 4], and (ii) anoxygenic photosynthesis in which bacteria could use $Fe(II)_{aq}$ instead of H_2O as the electron donor to produce the oxidized byproduct Fe(III) rather than gaseous oxygen [5, 6]. However, compared to these alternative mechanisms, UV photo-oxidation does not require involvement of any gaseous oxygen or biology, and the oxidation rate has been calculated to be high enough to account for the extensive occurrence of BIFs [2, 7].

The principal argument against photo-oxidation is based on the experimental observation that $Fe(II)_{aq}$ in solution tends to combine with bicarbonate and silicon to form insoluble minerals [8], but the experimental setup may not have been completely relevant to the conditions that prevailed at that time and it posed instead the question of Fe(II) solubility regardless of the process responsible for its oxidation. There is no direct evidence for the involvement of biology in the formation of BIFs as they lack microfossils [9]. The only indirect evidence comes from carbon and iron stable isotope signatures of BIF-associated carbonates, which point to dissimilatory iron reduction associated with respiration of organic carbon [10, 11]. To examine the role of UV photo-oxidation in BIF formation and to differentiate between the three scenarios, we performed photo-oxidation lab experiments and analyzed the isotopic compositions of the products to a very high precision. In particular, the mass fractionation law governing the photo-oxidation process was investigated.

Methods. Our experimental procedure has already been described in detail previously [12] and so is only outlined here in brief. Oxygen is evacuated from a closed reaction system with high-purity Ar gas (O_2 < 0.1 ppm). The system consists of a reactor containing 350 mL H_3BO_3-NaOH buffer, and an iron introduction section and a sampling section, both connected to the reactor. Ferrous iron as $(NH_4)_2Fe(SO_4)2.6H_2O$ salt is dissolved in absence of oxygen and $Fe(II)_{aq}$ is transferred to the reactor before the UV lamp is turned on. During the reaction, products are taken at 30 min time intervals. For each, product Fe(III) precipitate and $Fe(II)_{aq}$ solution are separated from each other with a 0.1 μm syringe filter.

Experiments for iron and oxygen isotope analyses were performed seperately. For iron analysis (experiment #1; [12]), the volume of each sampled $Fe(II)_{aq}$ − Fe(III) precipitate mixture was about 7 mL (not enough for oxygen isotope measurement). Oxygen was measured on Fe(III) precipitate in experiment #2, which was similar to the experiment #1 except that more iron was introduced and larger aliquots of 18 mL were sampled. Both Fe(III) solid and $Fe(II)_{aq}$ solution from experiment #2 were also analyzed for their iron isotopic composition. The iron isotopic composition was measured with a Thermo Scientific Neptune Plus MC-ICPMS at the university of Chicago as described in [13], while the oxygen isotope measurements were performed at the Open University using the procedures outlined by [14].

Results. Preliminary data of iron isotope analysis (δ-values in experiment #1) have been reported previously [12], the data show that the Fe(III) precipitate is enriched in heavier iron isotopes relative to the initial composition, while the $Fe(II)_{aq}$ solution has a lighter composition, and all of them plot on a mass-dependent isotope fractionation line. The newly obtained data, acquired in order to determine the iron isotope fractionation law during photo-oxidation, are expressed as ε'- values ($\varepsilon'^{i}Fe = 10000 * \ln(R_{i/54}/R_{i/54,\,std})$). The most fractionated samples have non-zero ε'- values. Since the ε'- values were calculated by normalizing $^{57}Fe/^{54}Fe$ ratio to a fixed value of 0.3625492 using the exponential law, the non-zero values indicate that the photo-oxidation process follows a mass fractionation law that differs from the exponential law.

For the experiment #2, there is no clear correlation between iron and oxygen isotopic compositions. The change of iron isotopic composition as a function of time follows the same trend as in the experiment #1 [12]. Oxygen isotopic composition of the precipitate is heavier (ranges from -0.14‰ to +0.80‰ with an average of +0.33‰ in terms of $\delta^{18}O_{VSMOW}$) compared to Chicago tap water which is about -0.5‰ [15].

Discussion. The δ-values of photo-oxidation experiment #1 follow a Rayleigh distillation model with an isotope fractionation factor of 1.0012, that is,

+1.2‰ instantaneous isotope fractionation between Fe(III) precipitate and $Fe(II)_{aq}$ solution at 45 ℃ [12]. A plot of $\varepsilon'^{56}Fe$ *vs.* $\delta'^{57}Fe$ (calculated as 1000*ln ($\delta^{57}Fe/1000 + 1$)) shows that the products of photo-oxidation follow the equilibrium law (n=-1) within error. Data with high enough precision is missing to compare the mass-fractionation law documented here with the other two processes (O_2-mediated oxidation and anoxygenic photosynthesis) that could have been involved in BIF formation, but it is likely that those would follow the equilibrium law as well.

The BIF sample measured at very high precision, IF-G, agrees with the experimental Fe(III) precipitate and the equilibrium law. However, in the experiments the data points providing better leverage in determining the law are $Fe(II)_{aq}$ solution. The counterpart to $Fe(II)_{aq}$ solution during BIF formation would be seawater, the composition of which may have been recorded in shales [16]. If that is true, measuring shales would be a promising way to further test the photo-oxidation hypothesis.

Unlike iron, where the solution and precipitate evolved in the course of photo-oxidation, no systematic trend of $\delta^{18}O$ as a function of time is seen, implying that the solution effectively acted as an infinite reservoir in terms of oxygen. The oxygen isotopic composition is consistent with equilibrium isotope fractionation between Fe(III) oxides and waters from previous experiments which found little fractionation (Fig. 1). Although it has been well known that UV light irradiation can cause photo-chemical reactions featuring mass-independent isotope fractionation, such as photolysis of ozone [17] and of SO_2 [18], no clear mass-independent isotope signature was found for photo-oxidation. The $\Delta^{17}O$ values of Fe(III) precipitate (calculated from measured δ-values) range between -0.133‰ and -0.048‰ with an average of -0.078‰, where the reference mass fractionation line is the terrestrial fractionation line with a slope of 0.5247 [19], are not outside the range of terrestrial materials.

In conclusion, the isotopic compositions of iron and oxygen measured in BIFs are consistent with the results from photo-oxidation experiments and therefore photo-oxidation remains a viable pathway to BIF formation.

References: [1] Cairns-Smith A. G. (1978) *Nature, 276,* 807–808. [2] Braterman P. S. et al. (1983) *Nature, 303,* 163–164. [3] Cloud P. E. (1965) *Science, 148,* 27–35. [4] Cloud P. (1973) *Econ. Geol., 68,*1135–1143. [5] Garrels R. M. et al. (1973) *Econ. Geol., 68,* 1173–1179. [6] Widdle F. (1993) *Nature, 362,* 834–836. [7] Francois L. M. (1986) *Nature, 320,* 352–354. [8] Konhauser K. O. et al. (2007) *EPSL, 258,* 87–100. [9] Klein C. (2005) *Am. Mineral., 90,*1473–1499. [10] Craddock P. R. and Dauphas N. (2011) *EPSL, 303,* 121–132. [11] Heimann A. et al. (2010) *EPSL, 294,* 8–18. [12] Nie N. X. and Dauphas N. (2015) *LPS 46,* #2635. [13] Dauphas N. and Rouxel O. (2006) *Mass Spectrom. Rev., 25,* 515-550. [14] Miller M. F. (1999) *Rapid Commun. Mass Spectrom. 13,* 1211-1217. [15] Bowen G. J. et al. (2007) *Water Resour. Res., 43(3).* [16] Rouxel O. J. et al. (2005) *Science, 307,* 1088-1091. [17] Chakraborty S. and Bhattacharya S. K. (2003) *J. Chem. Phys., 118,* 2164-2172. [18] Farquhar J. et al. (2001) *J. Geophys. Res., 106,* 32829-32839. [19] Miller M. F. (2002) *GCA, 66,* 1881-1889. [20] Frierdich A. J. et al. (2015) *GCA, 160,* 38-54. [21] Yapp C. J. (2007) *GCA, 71,*1115-1129. [22] Bao H. and Koch P. L. (1999) *GCA, 63,* 599-613. [23] Zheng Y. (1991) *GCA, 55,* 2299-2307.

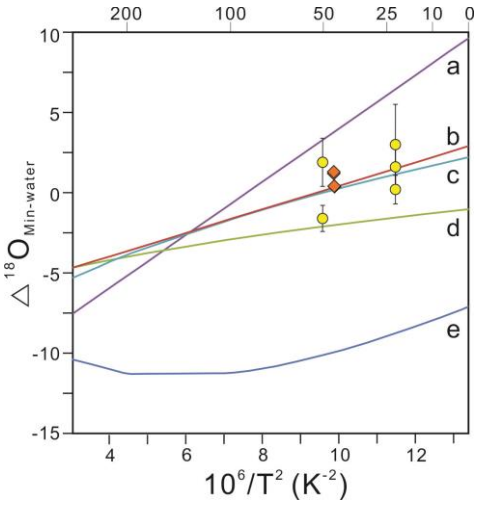

Fig. 1: *Oxygen isotopic fractionation between Fe(III) minerals and water. Yellow points are experimental data of geothite [20] and orange squares are from this study. Lines a, b, c, and d are experimental determinations while e is a theoretical calculation. a. Goethite [21]; b. Hematite [22]; c. Akaganeite [22]; d. Goethite [22]; e. Hematite [23].*